

Theoretical Study on Resonant Inelastic X-Ray Scattering in Quasi-One-Dimensional Cuprates

Takuji NOMURA* and Jun-ichi IGARASHI

Synchrotron Radiation Research Center, Japan Atomic Energy Research Institute, Mikazuki, Sayo, Hyogo 679-5148

(Received)

We study theoretically the resonant inelastic x-ray scattering in quasi-one-dimensional insulating copper oxides, where the incident photon energy is tuned to the $\text{Cu}1s$ - $4p$ absorption energy. Our attention is focused particularly on the strong momentum-transfer dependence of the spectral shape observed in recent experiments. We describe the antiferromagnetic ground state within the Hartree-Fock theory, and consider charge excitations from the ground state within the random phase approximation. By taking account of the electron correlation effects perturbatively, we obtain detailed momentum-transfer dependence of the spectra in a semi-quantitative agreement with the experiments.

KEYWORDS: Resonant inelastic x-ray scattering, One-dimensional copper oxide, Sr_2CuO_3 , SrCuO_2

Resonant inelastic x-ray scattering (RIXS) measurements are now becoming a promising and unique experimental technique to clarify the detailed charge excitation spectra of solids in a relatively high-energy range,¹ owing to high brilliance of synchrotron radiation. In particular, the RIXS measurements in the hard x-ray regime could be a new powerful tool to detect momentum dependent charge excitations in solids. A number of compounds have been investigated by this technique.²⁻⁹ Among them, the RIXS in cuprates utilizing the $\text{Cu}1s$ - $4p$ absorption edge attracts much interest recently, since relatively large momentum dependence was indeed observed in the charge excitation spectra.^{3-7,9}

The electronic properties of the quasi-one-dimensional (Q1D) insulating cuprates Sr_2CuO_3 (SCO213) and SrCuO_2 (SCO112) are well characterized by the one-dimensional chain consisting of the Cu-O plaquettes. The Cu-O chains are expected only weakly coupled with each other.¹⁰ In SCO213 the Cu-O plaquettes are aligned with sharing the corner oxygen atoms with the nearest plaquettes, as shown in Fig. 1. It was reported that SCO213 shows antiferromagnetic order below about 5 K with reduced staggered magnetization along the chain. The strong fluctuations are responsible for the extremely reduced Néel temperature and magnetization,¹¹ but the ground state of SCO213 is an antiferromagnetic (AF) insulator. Concerning SCO112, the Cu-O plaquettes form a zigzag chain by sharing the edges with the nearest plaquettes. The zigzag chain can be regarded approximately as being constructed by combining two independent Cu-O chains sharing the edges with each other.¹⁰ Therefore we study the RIXS properties of these two cuprates by considering the corner-sharing Cu-O chain as in Fig. 1 in the present article.

Recently, RIXS measurements were performed for the Q1D cuprates SCO213⁶ and SCO112.^{6,9} In the both Q1D cuprates, characteristic spectral weight was obtained for energy transfer $\omega \approx 2, 5.6$ (eV), but the origin of the spectral peaks are still unclear. The aim of the present

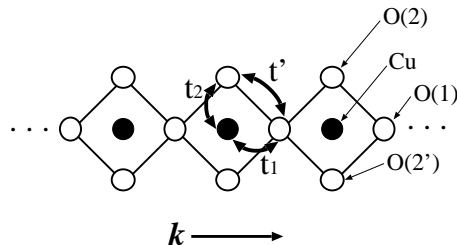


Fig. 1. Schematic figure of the Cu-O chain presenting the definition of the transfer integrals.

article is to provide a quantitative understanding on the RIXS, particularly on the position of the peaks and the highly momentum-dependent behaviors of the spectra in these one-dimensional cuprates. We calculate the intensity in the RIXS spectra as a function of energy-momentum transfer, using the perturbation theory developed by Platzman and Isaacs.¹⁴ We describe the antiferromagnetic (AF) ground state by the Hartree-Fock (HF) theory, and take account of the excitations from the ground state within the random phase approximation (RPA). As a result, we obtain a semiquantitative agreement with experiments, regarding the peak positions and the momentum dependent behaviors.

The essential microscopic process of the RIXS in the cuprates is considered to be as follows.¹² The incident photon excites resonantly the $\text{Cu}1s$ core electrons to the upper empty $\text{Cu}4p$ bands. Since the core $\text{Cu}1s$ orbitals are well localized to be coupled strongly to the $\text{Cu}3d$ electrons by the interorbital Coulomb interaction, the created $\text{Cu}1s$ core hole scatters the $\text{Cu}3d$ electrons, which occupy the bands relatively close to the chemical potential (As a result of the scattering, the most probably only one electron-hole pair is created on the $\text{Cu}3d$ band). In order to describe this process specifically, we consider the total Hamiltonian of the form, $H = H_{dp} + H_{1s-3d} + H_{1s} + H_{4p} + H_x$. The dp -Hamiltonian H_{dp} describing the electronic properties of the $\text{Cu}3d$ - $\text{O}2p$ bands is given in the form, $H_{dp} = H_0 + H'$. H_0 and H'

*E-mail: nomurat@spring8.or.jp

are the noninteracting and the interaction parts, respectively.

$$H_0 = \sum_{k\sigma} \mathbf{d}_{k\sigma}^\dagger \begin{pmatrix} \varepsilon_d & \zeta_1(k) & t_2 & -t_2 \\ -\zeta_1(k) & \varepsilon_{p1} & \zeta'(k) & -\zeta'(k) \\ t_2 & -\zeta'(k) & \varepsilon_{p2} & 0 \\ -t_2 & \zeta'(k) & 0 & \varepsilon_{p2} \end{pmatrix} \mathbf{d}_{k\sigma}, \quad (1)$$

where $\mathbf{d}_{k\sigma} = (d_{k\sigma}, p_{1k\sigma}, p_{2k\sigma}, p_{2'k\sigma})$, and $d_{k\sigma}, p_{1k\sigma}, p_{2k\sigma}$ and $p_{2'k\sigma}$ are the electron annihilation operators in the atomic $d_{x^2-y^2}$ or $p_{x,y}$ orbitals at the Cu, O(1), O(2) and O(2') atoms, respectively. The dispersions are $\zeta_1(k) = 2it_1 \sin \frac{k}{2}$ and $\zeta'(k) = 2it' \sin \frac{k}{2}$. The hopping parameters are $t_1 = -1.45$ eV, $t_2 = -1.8$ eV and $t' = -0.7$ eV (See Fig. 1), as determined for SCO213 by the LDA first principle calculation.¹³ The interacting part is

$$H' = \frac{U_d}{N} \sum_{kk'q} d_{k-q\uparrow}^\dagger d_{k'+q\downarrow}^\dagger d_{k'\downarrow} d_{k\uparrow}. \quad (2)$$

The Coulomb energy is taken to be $U_d = 11$ eV in the present study. Regarding the one-particle level, we take $\varepsilon_{p2} - \varepsilon_{p1} = 0.5$ eV, $\varepsilon_d^{\text{HF}} - \varepsilon_{p1} = -0.5$ eV, where $\varepsilon_d^{\text{HF}}$ is the screened Cu3d one-electron energy within the HF theory. For this parameters, we obtain the AF ground state with the staggered magnetization $m_{\text{stag.}} = 0.43\mu_B$. The scattering of the Cu3d electrons by the Cu1s core hole is described by

$$H_{1s-3d} = \frac{V}{N} \sum_{kk'q\sigma\sigma'} d_{k'+q\sigma}^\dagger s_{k-q\sigma'}^\dagger s_{k\sigma'} s_{k\sigma} d_{k'\sigma}, \quad (3)$$

where $s_{k\sigma}$ ($s_{k\sigma}^\dagger$) is the annihilation (creation) operator for the Cu1s electrons with momentum k and spin σ , and V is the so-called core-hole potential. H_{4p} and H_{1s} describe the kinetics of the electrons on the Cu4p and Cu1s bands. Since the Cu1s electrons are well localized, we take completely flat dispersion for them. For the Cu4p electrons, we use simple two-dimensional cosine-shaped band for simplicity. This simplification does not affect the spectral shape so drastically, because the factor containing the Cu4p dispersion function is integrated up in momentum, as seen later in eq. (5). H_x describes the transitions between the Cu1s and Cu4p states, involving the photon absorption and inverse emission processes. H_x is of the form

$$H_x = \sum_{kq\sigma} (w(q; k) p_{k+q\sigma}^\dagger s_{k\sigma} + \text{h.c.}), \quad (4)$$

where p^\dagger is the creation operator of the Cu4p electron. In the present study, we ignore the momentum dependence of the matrix elements $w(q; k)$, i.e., $w(q; k) = w$.

The main spectral weight of the RIXS is evaluated by the diagram shown in Fig. 2. In Fig. 2(a), the effective three point vertex function $\Lambda(\omega, q)$ represented by the shaded triangle is calculated within the RPA, and this vertex part is inserted to the diagram Fig. 2(b) representing the total scattering probability. In Fig. 2(b), note that the off-diagonal components of the Keldysh Green's functions are assigned to the solid lines which connect the upper normally-time-ordered branch and the lower reversely-time-ordered branch, while the usual causal (normally-time-ordered) Green's functions are assigned to the solid lines in the upper branch and the

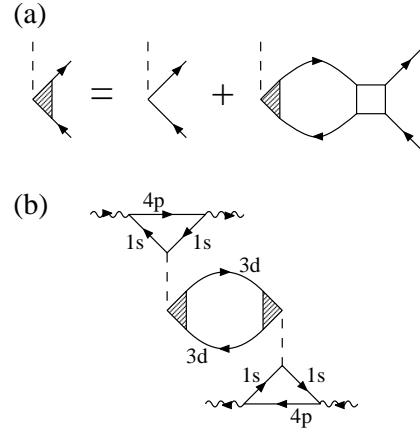


Fig. 2. (a) Vertex renormalization in the RPA. The solid lines, the shaded triangle and the empty square are the Green's function for Cu3d electrons, the renormalized vertex and the anti-symmetrized bare Coulomb interaction, respectively. (b) The diagrammatic representation of the RIXS intensity. The wavy and the dashed lines denote photons and the 1s-core-hole potential, respectively. The Green's functions for Cu3d, Cu1s and Cu4p electrons are assigned to the solid lines marked with '3d', '1s' and '4p', respectively.

reversely-time-ordered Green's functions are assigned to the solid lines in the lower branch.¹⁵ Regarding the core hole potential V , we take only the first order term in V (i.e., Born scattering). The effect of higher orders in V is briefly mentioned later. The analytic expression for the diagram Fig. 2(b) is obtained as

$$W(\omega_i q_i; \omega_f q_f) = (2\pi)^3 N |w|^4 \sum_{kjj'} \delta(E_j(k) + \omega - E_{j'}(k+q)) \times n_j(k)(1 - n_{j'}(k+q)) \left| \sum_{\sigma\sigma'} U_{j,d\sigma}(k) \Lambda_{\sigma\sigma'}(\omega, q) U_{d\sigma',j'}^\dagger(k+q) \times \sum_{k_1} \frac{V}{(\omega_i + \varepsilon_{1s} + i\Gamma_{1s} - \varepsilon_{4p}(k_1))(\omega_f + \varepsilon_{1s} + i\Gamma_{1s} - \varepsilon_{4p}(k_1))} \right|^2, \quad (5)$$

where q_i and q_f (ω_i and ω_f) are the momenta (energies) of the initially absorbed and the finally emitted photons, respectively. $q = q_i - q_f$ and $\omega = \omega_i - \omega_f$ are the momentum transfer and the energy loss, respectively. $E_j(k)$ and $n_j(k)$ are the energy dispersion and the electron occupation number of the band j , respectively, obtained by diagonalizing the HF Hamiltonian for H_{dp} . $U_{j,d\sigma}(k)$ is the $(j, d\sigma)$ -element of the unitary matrix diagonalizing the HF Hamiltonian for H_{dp} . ε_{1s} and $\varepsilon_{4p}(k)$ are the kinetic energies of the Cu1s and Cu4p electrons, respectively. In the present study the incident photon energy ω_i is tuned to the Cu1s-4p absorption energy $\omega_i \approx \varepsilon_{4p}(0) - \varepsilon_{1s}$, for which the intensity of the spectrum is enhanced by the resonance. The decay rate Γ_{1s} of the core hole is 0.8 eV in the present study.

The numerical results of the RIXS intensity by the formula eq. (5) are shown as a function of energy loss ω for momentum transfers $q = 0, \frac{\pi}{2}$ and π in Fig. 3. We see that there are three characteristic peaks in the calculated RIXS spectra around $\omega \approx 2, 6, 10$ eV. In the experiments, two peaks are observed around the momentum transfer $\omega \approx 2$ and 5.6 eV, which are in agreement with the present numerical results. The high-energy 10eV

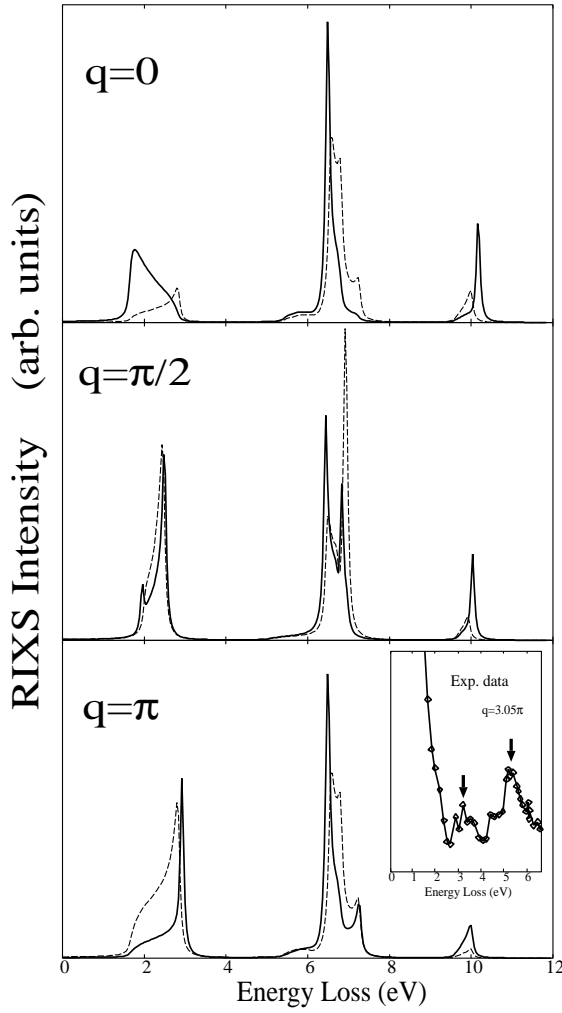


Fig. 3. The calculated spectra as a function of energy loss for three momentum transfers $q = 0, 0.5\pi$ and π . The thick solid and the thin broken lines are the results with and without the RPA corrections, respectively. The inset shows a typical experimental spectrum read from ref. 6, and the arrows point the two peaks.

peak gives only small contribution to the total spectral weight, and the intensity around $\omega \approx 2$ and 6 eV covers the main part of the spectral weight. In Fig. 4, the contourplots of the calculated RIXS spectra are shown as a function of the momentum transfer q and the energy loss ω , and the experimental data read from ref. 6 are also displayed for comparison. We can see that the 2eV peak shows a relatively large sinusoidal dispersion, while the other two do not. This sinusoidal dispersion of the 2eV peak quantitatively agrees with the experiments.^{6,9} Concerning the 6eV peak, the calculated peak positions deviate somewhat from the experimental ones, maybe due to the crude tight-binding fitting. The weak momentum dependence of the 6eV peak position is well reproduced by the calculation.

In order to inspect the origin of the peaks in the RIXS spectra, we should turn back to the formula (5). Comparing the results modified by the correlations (the solid lines in Fig. 3) with the uncorrected results (the dashed lines in Fig. 3), we can see that the overall spectral shape is roughly captured even without any correlation effects,

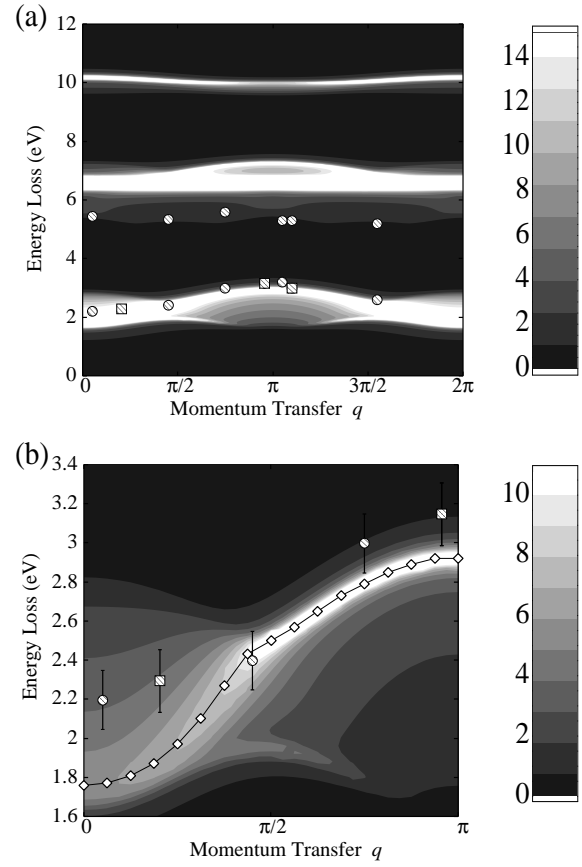


Fig. 4. Graylevel plots for the spectra as a function of momentum transfer and energy loss. The light and dark regions correspond to high and low RIXS intensity, respectively. The hatched squares and circles are experimental peak positions in SCO213 and SCO112, respectively, from ref. 6. In (b), the diamonds connected by a thin line denote the theoretical peak positions.

although the detailed spectral structure are of course affected by the correlation effects. Therefore we might expect that the overall spectral shape is determined by the other factors rather than the correlation effects on the scattering process, and thus expect naturally that the factor $n_j(k)(1 - n_{j'}(k+q))|U_{j,d\sigma}(k)U_{d\sigma',j'}^\dagger(k+q)|^2$ is essential for determining the overall spectral shape. It is very interesting to note that this factor is the product of the partial electron occupation number of the band j at the momentum k [$n_j(k)|U_{j,d\sigma}(k)|^2$] and the partial hole occupation number of the band j' with the momentum $k+q$ [$(1 - n_{j'}(k+q))|U_{d\sigma',j'}^\dagger(k+q)|^2$]. Thus the Cu1s-4p RIXS spectra in cuprates are closely related to the partial occupation number of the Cu3d electrons in each band. From this point of view, the RIXS spectra reflect the charge excitation processes in which Cu3d electrons are selectively excited from the lower occupied bands to the upper unoccupied bands. In Fig. 5, the total and the Cu3d partial density of states (DOS) are shown. We find only one DOS weight around $\omega \approx 1$ eV above the chemical potential, and four DOS weights around $\omega \approx -2, -4, -6, -9$ eV below the chemical potential. We can consider naturally that the three RIXS weights around 2, 6 and 10 eV in Fig. 3 are attributable to the excitation processes in which the electrons occupying the

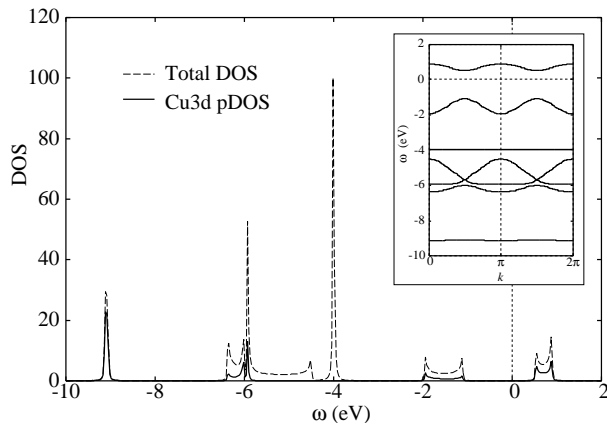


Fig. 5. The density of states for the antiferromagnetic ground state. The thin dotted and thick solid lines represent the total and the Cu3d partial density of states, respectively. The chemical potential is set to $\omega = 0$. The inset shows the band dispersions.

bands $\omega \approx -2, -6$, and -9 eV are excited to the upper unoccupied band. Of interest is that the sharp peak in the total DOS around $\omega \approx -4$ eV, which corresponds to the non-bonding oxygen band, is not reflected in the RIXS spectra at all. This is because the oxygen non-bonding band does not contain any components of the Cu3d orbitals and the other orbitals which are enough localized at the Cu-sites to be coupled strongly to the Cu1s orbitals. In this sense, the Cu1s-4p RIXS measures the Cu3d-orbital-selective charge excitations. In general, only the bands which are hybridized with the localized orbitals strongly coupled to the core hole are observable in the RIXS spectra.

We should make a distinction between the 2, 6 eV peaks and the 10 eV peak in the RIXS spectra (Fig. 3). Since the DOS peaks around $\omega \approx 1$ and -9 eV correspond respectively to the upper and lower Hubbard bands, the RIXS spectral weight around 10 eV in Fig. 3 is related to the charge excitation process across the Mott-Hubbard energy gap, which is usually of the order of U_d . On the other hand, the RIXS spectral weights around 2 and 6 eV are related to the charge transfer (CT) process in which the Cu3d electrons mixed in the wide O2p bands are excited to the upper empty Cu3d Hubbard band. This energy scale of the CT excitation is basically connected to the CT energy $\varepsilon_p - \varepsilon_d$. We should note that the main spectral weight originates from the CT process, and the excitations across the Mott-Hubbard gap provides only minor contribution to the RIXS spectra. Therefore, the validity of the theoretical analyses based on the single-band Hubbard model,¹² which consider only Cu sites, is unclear.

We give some remarks on the present calculations. At first, we discuss the validity of the application of the HF theory to the present system. Although the experiments are usually performed above the Néel temperature, the HF analysis is valid in principle only at the absolute zero temperature. In actual low-dimensional systems including the cuprates, the fluctuations are very strong to reduce the Néel temperature and the magnitudes of order parameters. However we would like to stress that it is

not so important for the RIXS spectra whether the AF long range order is attained or only short range AF correlation exists. The reasons are as follows. (i) The AF transition does not affect the RIXS spectra so drastically, since the RIXS spectra basically reflect only the charge sector in the scattering process. (ii) The RIXS occurs, basically being well localized in the space, due to the localized nature of the Cu1s core hole. In addition to these points, by noting that the AF ground states in Mott insulators may be continued adiabatically to the HF AF ground state at the absolute zero temperature in the limit of strong Coulomb repulsion, we consider that the AF HF theory provides a good starting point to the analysis.¹⁶ But we should note here the following point. As we have mentioned, the RIXS spectral weight is roughly determined by the product of the Cu3d partial occupation numbers in the occupied and the unoccupied bands. Since the HF theory usually underestimates the magnitude of the localized moment, the product of Cu3d electron and hole occupation numbers $n_{i\sigma}(1 - n_{i\sigma})$ in the local picture is overestimated. Thus the intensity around 10 eV in the RIXS spectra is overestimated within the HF theory. It is natural to consider that the CT excitations, rather than the charge excitation process across the Mott-Hubbard gap, provide the main contribution to the spectral weight, and the 10 eV peak might not be observable in reality.

We have considered only the first order terms in the core hole potential V . Actually we investigated the effects of higher orders in V within the T -matrix approximation as in usual single impurity problems (Results are not shown). However we found that the spectral shape is not so drastically changed by the higher orders of V , although the absolute magnitude of the spectra is changed.

In the present work, we have analyzed theoretically the RIXS spectra in the Q1D cuprates. The peak positions and the momentum-transfer dependence of the RIXS spectra are explained in a semiquantitative agreement with the experimental results. We have shown that the RIXS measurement in cuprates is a unique technique to clarify the Cu3d-orbital-selective charge excitations.

The authors are much grateful to Prof. M. Hasan for the communications. The numerical computation was partly performed at the Yukawa Institute Computer Facility.

- 1) A. Kotani and S. Shin: Rev. Mod. Phys. **73** (2001) 203.
- 2) C. -C. Kao *et al.*: Phys. Rev. B **54** (1996) 16361.
- 3) J. P. Hill *et al.*: Phys. Rev. Lett. **80** (1998) 4967.
- 4) P. Abbamonte *et al.*: Phys. Rev. Lett. **83** (1999) 860.
- 5) M.Z. Hasan *et al.*: Science **288** (2000) 1811.
- 6) M.Z. Hasan *et al.*: Phys. Rev. Lett. **88** (2002) 177403.
- 7) Y. J. Kim *et al.*: Phys. Rev. Lett. **89** (2002) 177003.
- 8) T. Inami *et al.*: Phys. Rev. B **67** (2003) 045108.
- 9) Y. J. Kim *et al.*: cond-mat/0307497.
- 10) N. Motoyama *et al.*: Phys. Rev. Lett. **76** (1996) 3212.
- 11) K. M. Kojima *et al.*: Phys. Rev. Lett. **78** (1997) 1787.
- 12) K. Tsutsui *et al.*: Phys. Rev. Lett. **61** (2000) 7180.
- 13) R. Neudert *et al.*: Phys. Rev. B **62** (2000) 10752.
- 14) P. M. Platzman and E. D. Isaacs: Phys. Rev. B **57** (1998) 11107.
- 15) P. Nozières and E. Abrahams: Phys. Rev. B **10** (1974) 3099.
- 16) N. Bulut *et al.*: Phys. Rev. Lett. **73** (1994) 748.